

## Overview of Recent Work on Laser Excitation of Positronium for the Formation of Antihydrogen

P. Yzombard<sup>1</sup>, C. Amsler<sup>2</sup>, T. Ariga<sup>2</sup>, G. Bonomi<sup>3,4</sup>, P. Bräunig<sup>5</sup>, R. S. Brusa<sup>6,7</sup>, L. Cabaret<sup>1</sup>, M. Caccia<sup>8</sup>, R. Caravita<sup>9,10,14</sup>, F. Castelli<sup>8,11</sup>, G. Cerchiarri<sup>12</sup>, D. Comparat<sup>1</sup>, G. Consolati<sup>8,13</sup>, A. Demetrio<sup>5</sup>, L. Di Noto<sup>9,10</sup>, M. Doser<sup>14</sup>, A. Ereditato<sup>2</sup>, C. Evans<sup>8,13</sup>, R. Ferragut<sup>8,13</sup>, J. Fesel<sup>14</sup>, A. Fontana<sup>4</sup>, S. Gerber<sup>14</sup>, M. Giammarchi<sup>8</sup>, A. Gligorova<sup>15</sup>, F. Guatieri<sup>6,7</sup>, S. Haider<sup>14</sup>, H. Holmestad<sup>16</sup>, T. Huse<sup>16</sup>, A. Kellerbauer<sup>12</sup>, D. Krasnický<sup>9,10</sup>, V. Lagomarsino<sup>9,10</sup>, P. Lansonneur<sup>17</sup>, P. Lebrun<sup>17</sup>, C. Malbrunot<sup>14,18</sup>, S. Mariazzi<sup>18</sup>, V. Matveev<sup>19,20</sup>, Z. Mazzotta<sup>8,11</sup>, G. Nebbia<sup>21</sup>, P. Nedelec<sup>17</sup>, M. Oberthaler<sup>5</sup>, N. Pacifico<sup>15</sup>, D. Pagano<sup>3,4</sup>, L. Penasa<sup>6,7</sup>, V. Petracek<sup>22</sup>, C. Pistillo<sup>2</sup>, F. Prelz<sup>8</sup>, M. Prevedelli<sup>23</sup>, L. Ravelli<sup>6,7</sup>, B. Rienaecker<sup>14</sup>, O.M. Røhne<sup>16</sup>, A. Rotondi<sup>4,24</sup>, M. Sacerdoti<sup>8,11</sup>, H. Sandaker<sup>16</sup>, R. Santoro<sup>8,25</sup>, P. Scamporrì<sup>2,26</sup>, L. Smestad<sup>14,27</sup>, F. Sorrentino<sup>9,10</sup>, I. M. Strojek<sup>22</sup>, G. Testera<sup>10</sup>, I. C. Tietje<sup>14</sup>, S. Vamosi<sup>18</sup>, E. Widmann<sup>18</sup>, J. Zmeskal<sup>18</sup>, N. Zurlo<sup>4,28</sup>

<sup>1</sup>Laboratoire Aimé Cotton, Université Paris-Sud, ENS Cachan, CNRS, Université Paris-Saclay, 91405 Orsay Cedex, France

<sup>2</sup>Laboratory for High Energy Physics, Albert Einstein Center for Fundamental Physics, University of Bern, 3012 Bern, Switzerland

<sup>3</sup>Department of Mechanical and Industrial Engineering, University of Brescia, via Branze 38, 25123 Brescia, Italy

<sup>4</sup>INFN Pavia, via Bassi 6, 27100 Pavia, Italy

<sup>5</sup>Kirchhoff-Institute for Physics, Heidelberg University, Im Neuenheimer Feld 227, 69120 Heidelberg, Germany

<sup>6</sup>Department of Physics, University of Trento, via Sommarive 14, 38123 Povo, Trento, Italy

<sup>7</sup>TIFPA/INFN Trento, via Sommarive 14, 38123 Povo, Trento, Italy

<sup>8</sup>INFN Milano, via Celoria 16, 20133, Milano, Italy

<sup>9</sup>Department of Physics, University of Genova, via Dodecaneso 33, 16146 Genova, Italy

<sup>10</sup>INFN Genova, via Dodecaneso 33, 16146 Genova, Italy

<sup>11</sup>Department of Physics, University of Milano, via Celoria 16, 20133 Milano, Italy

<sup>12</sup>Max Planck Institute for Nuclear Physics, Saupfercheckweg 1, 69117 Heidelberg, Germany

<sup>13</sup>Politecnico di Milano, Piazza Leonardo da Vinci 32, 20133 Milano, Italy

<sup>14</sup>Physics Department, CERN, 1211 Geneva 23, Switzerland

<sup>15</sup>Institute of Physics and Technology, University of Bergen, Allégaten 55, 5007 Bergen, Norway

<sup>16</sup>Department of Physics, University of Oslo, Sem Saelandsvei 24, 0371 Oslo, Norway

<sup>17</sup>Institute of Nuclear Physics, CNRS/IN2p3, University of Lyon 1, 69622 Villeurbanne, France

<sup>18</sup>Stefan Meyer Institute for Subatomic Physics, Austrian Academy of Sciences, Boltzmannngasse 3, 1090 Vienna, Austria

<sup>19</sup>Institute for Nuclear Research of the Russian Academy of Science, Moscow 117312, Russia

<sup>20</sup>Joint Institute for Nuclear Research, 141980 Dubna, Russia

<sup>21</sup>INFN Padova, via Marzolo 8, 35131 Padova, Italy

<sup>22</sup>Czech Technical University, Prague, Brehovà 7, 11519 Prague 1, Czech Republic

<sup>23</sup>University of Bologna, Viale Berti Pichat 6/2, 40126 Bologna, Italy

<sup>24</sup>Department of Physics, University of Pavia, via Bassi 6, 27100 Pavia, Italy

<sup>25</sup>Department of Science, University of Insubria, Via Valleggio 11, 22100 Como, Italy

<sup>26</sup>Department of Physics Ettore Pancini, University of Napoli Federico II, Complesso Universitario di Monte S. Angelo, 80126, Napoli, Italy

<sup>27</sup>The Research Council of Norway, P.O. Box 564, NO-1327 Lysaker, Norway

<sup>28</sup>Department of Civil Engineering, University of Brescia, via Branze 43, 25123 Brescia, Italy

E-mail: [pauline.yzombard@u-psud.fr](mailto:pauline.yzombard@u-psud.fr)

(Received May 30, 2016)

The AEGIS experiment carried out at CERN aims to form a cold antihydrogen beam to perform precision studies on gravity. A key ingredient is the creation of antihydrogen via a charge-exchange process between trapped antiprotons and Rydberg excited positronium atoms (Ps). In the present, the latest results of laser excitation of Ps are reviewed, as well as studies on a possible laser manipulation and cooling of Ps and antiprotons.

**KEYWORDS:** Positronium, Antihydrogen, Laser-matter interaction, Positronium laser excitation, Positronium laser cooling, anions laser cooling

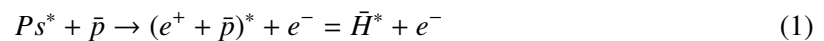
## 1. Introduction

Since its prediction by Dirac at the beginning of the past century and its first experimental discovery in 1932 by Anderson, antimatter has generated great interest and triggered multiple studies, among which experimental tests on the QED theory [1], the CPT theorem and the Weak Equivalence Principle (WEP). The WEP states that any body in a gravitational field experiences the same acceleration, independent of its own composition. Several tests verified the WEP at  $10^{-13}$  accuracy for ordinary matter [2], and some experiments [3, 4] and theoretical discussions [5] infer that the WEP should hold for antimatter ; however, this statement relies on theoretical assumptions and indirect arguments. Moreover, several attempts to model a quantum gravity theory tend to predict a possible violation of the WEP for antimatter [6], and further tests of the WEP are still required.

As the unique source of cold antiprotons in the world, the Antiproton Decelerator (AD) facility at CERN has provided bunches of tens of millions cold antiprotons (5.3 MeV  $\bar{p}$ ) for fourteen years. Antihydrogen atoms have been produced [7, 8] at few tens of Kelvin, and even a trapping technique has been developed to catch small numbers for several minutes [9]. These advances open paths for systematic studies of antimatter properties, as atomic spectroscopy or gravity tests. As the GBAR experiment [10] or the recent ALPHA-g project [11], the AEGIS collaboration [12] wants to investigate the effect of gravity on antimatter. More specifically, AEGIS aims to measure the deflection of a cold antihydrogen beam under Earth's gravitational field in order to perform a direct test of the WEP.

## 2. The AEGIS experiment

The AEGIS collaboration expects to form antihydrogen atoms using a 3-body charge-exchange process between trapped antiprotons and a Rydberg excited Ps cloud:



The formation of antihydrogen by charge-exchange process has already been done by the ATRAP collaboration [13]. In their system, the excitation of Ps toward a Rydberg state was performed using cesium atoms  $Cs^*$  excited by laser that collided with the Ps cloud. AEGIS rather plans to directly laser excite positronium.

The setup principle is shown in the Fig. 1. The antiprotons and positrons are separately trapped. After accumulation of positrons bunches, the  $e^+$  plasma is loaded via diocotron movement in an off-axis trap and shot toward a convertor target, where positronium atoms are emitted and enter in collision with the trapped  $\bar{p}$  to form antihydrogen.

One of the benefits of using such a process is the possibility to trigger the formation of antihydrogen, by controlling the positrons' implantation and consequently the time of formation of the

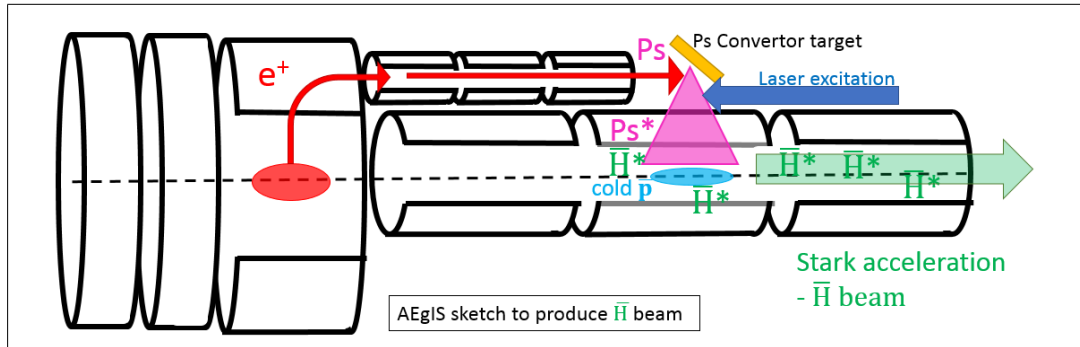


**Fig. 1.** Schematic of the AEgIS apparatus for antihydrogen beam formation. Positrons are shot onto a converter target, bind electrons and form Ps atoms. A Ps cloud is emitted, laser excited toward Rydberg states and then encounter the  $\bar{p}$  plasma, where the charge-exchange process can occur to create antihydrogen. Finally, a Stark acceleration will extract the  $\bar{H}$  from the high-magnetic field of the traps toward a free-field region, where the deflection measurement of the effect of gravity will take place.

incoming Ps cloud. This is crucial for a time-of-flight measurements as planned in AEgIS. In order to detect the vertical displacement of the  $\bar{H}$  trajectory, a classical (moiré) deflectometer will be used. The strength of gravity  $g$  for anti-atoms should be promptly extracted from these measurements [14].

Besides, the charge-exchange method forms  $\bar{H}$  with a narrow and well-defined  $n$ -state distribution, in comparison to the mixing process that is the other usual method to create  $\bar{H}$  [15]. Indeed, during the charge exchange, the formed  $\bar{H}$  has a similar binding energy as the internal energy of the Ps\* implicated in the reaction. This control in internal energies is of great interest for AEgIS, since a Stark acceleration is needed to extract and form the beam to perform the measurements outside the high magnetic field environment of the main trap.

In order to enhance the efficiency of the  $\bar{H}$  formation rate, the positronium atoms emitted from the converter target have to be excited toward Rydberg levels ( $n \geq 15$ ). In our setup, this is crucial for mainly two reasons: increasing the lifetime of Ps that have to cross the  $\sim 2$  cm distance between the target and the trapped  $\bar{p}$  plasma region, and enlarging the Ps collision cross section that scales as  $n^4$ .

In the present work, we would like first to quickly introduce the positron system and the positronium production in AEgIS, as well as the laser excitation pathway and setup. The most recent Ps laser excitation that we have obtained will be then shown. Finally, we would like to open the discussion by presenting two possible schemes using laser interactions to improve the  $\bar{H}$  formation in AEgIS.

### 3. Positronium formation in AEgIS

The AEgIS experiment holds two apparatuses: the main Penning-Malmberg traps at 4.5 T and 1 T, in cryogenic environment ; and a vacuum test chamber at room temperature. A schematic of the AEgIS zone is presented in Fig.2. The main traps are sited in the prolongation of the AD arm that provides the bunches of  $\bar{p}$ 's. In these traps the manipulation, compression and cooling of antiproton and positron plasmas, as well as the antihydrogen formation, take place. In contrast, the vacuum test chamber has been designed and built to study the  $e^+$  and Ps physics in a low-field region, with a tunable magnetic field from less than 2 Gauss up to 300 Gauss [16].

The positron system, mainly composed by a  $^{22}\text{Na}$  radioactive source and two Surko-like traps to cool and accumulate positrons can deliver positrons toward either the main apparatus or the test chamber. In spring 2015 when the measurements presented here have been performed, the source had an intensity of around 11mCi, and the system was able to typically provide bunches of  $8 \cdot 10^7 e^+$  every 3 minutes. In order to form positronium in AEGIS, after accumulation, positrons are accelerated to a few keV to be implanted into a silica-based nano-porous target, previously referred to as the convertor target in Fig. 1. Positrons diffuse into the silicon bulk of the convertor until reaching the silica-coated surface of the nano-channels where they bind with an electron and form Ps. If para-positronium (p-Ps) has a too short a lifetime to be emitted toward the surface (125 ps), ortho-positronium (o-Ps) experiences multiple collisions with the walls of the nano-channels and partially thermalizes before reaching the target surface and being emitted into vacuum with a lifetime of 142 ns.

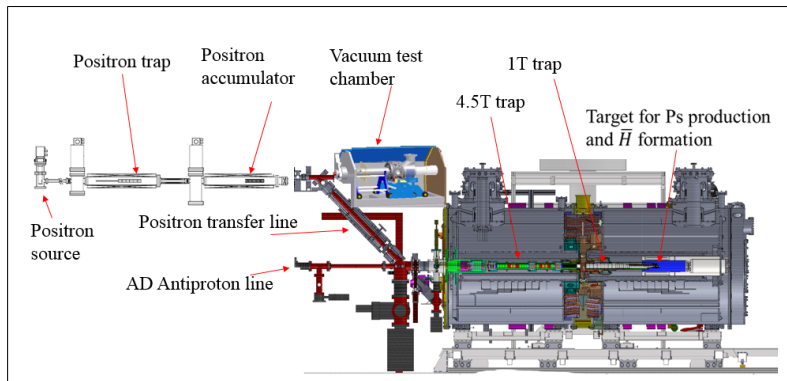


Fig. 2 Schematic of the AEGIS experimental zone, in front view. In the first floor, the AD arm provides  $\bar{p}$  that are trapped into the main apparatus (first in the 4.5 Tesla trap and then into the 1 Tesla trap). On the second floor, the positron system is installed, as well as the test chamber. A transfer line has been built to transport  $e^+$  from the accumulator traps into the main traps

Positronium emission is detected via a Single Shot Positron Lifetime Annihilation Spectrum technique (SSPALS) [17]. A  $\text{PbWO}_4$  scintillator ( $25 \times 25 \times 20 \text{ mm}^3$ ) coupled to a Hamamatsu R11265-100 PMT registers fast annihilation signals. Fig. 3 shows typical signals of  $e^+$  implantation and Ps formation inside the test chamber of AEGIS. The grey curve has been recorded from 10 positrons implantation shots in a micro-channel plate (MCP) placed instead of the convertor target. We observe a 2 gamma annihilation prompt peak. The black curve is the averaged signal of 10 shots of  $e^+$  implanted in the convertor target. The long tail part (distinguishable from the  $e^+$  prompt peak starting from 50 ns) is the annihilation signal of o-Ps emitted into vacuum, with a fit value of 140 ns [16].

#### 4. Ps laser excitation scheme in AEGIS

AEGIS aims to excite Ps around  $n=15$  to  $n=20$  to drastically improve the  $\bar{H}$  formation rate. In order to reach Rydberg states, a direct excitation from the o-Ps ground state can be considered, using a 182 nm laser beam. However, for both theoretical and technologies reasons, it has appeared to us to be more efficient to choose a two-photon absorption solution [19]. Although the production of Rydberg positronium has been first demonstrated by Cassidy and Mills ([18]), using a two-photon process via  $1^3\text{S} \rightarrow 2^3\text{P} \rightarrow n=\text{Rydberg}$  states, the AEGIS collaboration has preferred to design and build a laser system to reach Rydberg levels using the  $n=3$  state as the intermediate step. The excitation from  $n=3$  to Rydberg states is expected to be more efficient and to require less laser intensity than from  $n=2$  level [19], which is of interest when laser excitation has to be done in a cryogenic environment as in the AEGIS apparatus, where any warming-up from the lasers has to be avoided.

Briefly, a NdYAG Q-switched EKSPLA source provides pulses of the first, second and fourth

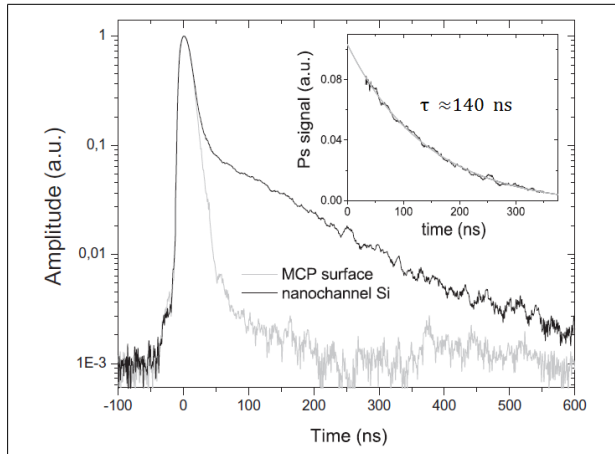


Fig. 3 Typical SSPALS spectra measurements. The grey curve shows the  $e^+$  prompt peak annihilation on an MCP and is used as a background signal (no Ps formation). In the black curve, positrons have been implanted in a convertor target to form Ps. After the prompt peak of  $e^+$  annihilation ( $t \geq 50$  ns), the long tail of the signal corresponds to o-Ps annihilation in vacuum, with an expected lifetime value of 142 ns. In the top right window image of the figure, a zoom shows the long tail annihilation signal, which is fit by a decreasing exponential with a  $\tau \sim 140$  ns.

Each curve is the average of 10 SSPALS signals.

harmonics to pump a non linear crystal based laser system and generates intense pulses of UV beam at 205 nm ( $1^3S \leftrightarrow 3^3P$  transition) and IR beam with a spectral range of 1675 nm - 1715 nm ( $3^3P \leftrightarrow$  Rydberg  $n= 15- 20$ ). These beams have been designed to be broadband enough (FWHM  $\approx 110$  GHz) to cover Doppler broadening and Zeeman splitting in the 1 T cryogenic environment of the main trap apparatus.

## 5. Ps laser excitation - some recent results

All the measurements presented here have been carried out in a 250 Gauss and -600 V/cm electromagnetic environment. Positrons have been implanted with 3.3 keV energy, for a cloud size of less than 4 mm (full width at tenth of maximum) and 7 ns of pulse width. In order to maximize the Ps laser excitation signal, a careful timing synchronization between positron implantation and laser shots has been controlled via a custom field-programmable gate array (FPGA) based device. The excitation lasers have been shined as close as possible to the convertor surface to optimize the geometric overlap of the emitted Ps cloud and the laser spots.

### 5.1 The first observation of the $n=3$ Ps laser-excited state

We first performed laser excitation of the  $n=3$  state of Ps at a moderate saturation regime, shining  $56 \mu\text{J}$  of the 205 nm light with a beam size of 4 mm  $\times$  6 mm. Its spectral bandwidth is about 110 GHz (FWHM), and the temporal FWHM of the pulse is about 1.5 ns. As a diagnostic, a highly saturated photoionization laser ( $\lambda_{ionization} = 1064$  nm) has been shot at the same time as the UV beam, that dissociates any Ps that was excited toward its  $n=3$  state. As a consequence, the laser excitation and photoionization is translated by the quasi-instantaneous destruction of Ps, and by a reduction of the number of o-Ps propagating in vacuum. In other words, the excitation + photoionization signals obtained show a consequent decrease of the annihilation counts in the tails of the SSPALS spectra. The fraction of S photoionized excited Ps atoms was evaluated from the area difference of the long-tail of the SSPALS spectra, recorded with ( $A_{ON}$ ) and without ( $A_{OFF}$ ) laser excitations, between 50 ns and 250 ns.

$$S(\%) = 100 \frac{A_{OFF} - A_{ON}}{A_{OFF}} \quad (2)$$

By varying the wavelength of the UV laser, we were able to perform a Doppler scan of the Ps velocity distribution. Measurements results are shown in Fig. 4 ; the central wavelength was found to be  $205.05 \pm 0.02$  nm, in good agreement with the theoretical value of 205.0474 calculated for

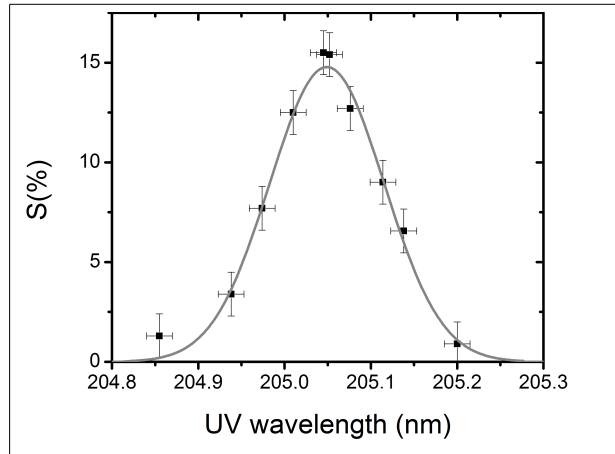


Fig. 4 The transition line of the  $1^3S \leftrightarrow 3^3P$ , obtained by scanning the frequency of the UV laser, for a constant energy of  $56 \mu\text{J}$ . The photoionization laser was set at  $50 \text{ mJ}$ , in the high saturation regime. Each point is the average of 15 SSPALS shots. The continuous curve is the result of a fit analysis that gives a Doppler broadening of the transition line corresponding to a mean transverse temperature of the Ps cloud of  $T \approx 1300 \pm 200 \text{ K}$ . result published in [20]

our electro-magnetic environment. At resonance, the maximum excitation signal we obtained was  $S(\delta = 0) = 15.5\%$ , where  $\delta = \omega_0 - \omega_L$  is the detuning of the laser compared to the transition frequency. Since the large linewidth measured for the  $n=1 \leftrightarrow n=3$  transition was mostly due to the Doppler broadening of the Ps cloud, we extracted a standard deviation of the o-Ps velocity in the transverse direction of  $10^5 \text{ m}\cdot\text{s}^{-1}$ , where meaning a temperature of  $T \approx 1300 \pm 200 \text{ K}$ . These results are in agreement with previous observations of partially-thermalized emission from similar targets at low implantation energy [21].

### 5.2 Rydberg excitations

We then carried out the Rydberg excitation measurements, replacing the photoionization laser by the dedicated IR beam to perform the  $n=3 \leftrightarrow n=15 - 18$  Rydberg state excitations. The UV beam was set at resonance at  $205.05 \text{ nm}$ , with a constant  $56 \mu\text{J}$  energy, and the IR beam frequency was scanned through  $\lambda_{Ryd} = 1685 - 1715 \text{ nm}$ , with an energy of  $1.2 \text{ mJ}$  and a spot size of  $8 \text{ mm}^2$  FWHM. The temporal pulse width is about  $4 \text{ ns}$  (FWHM), and its spectral FWHM is around  $110 \text{ GHz}$ .

Fig. 5 a) gives a typical averaged SSPALS spectrum, for laser excitation toward the  $n=15$  Rydberg state (grey curve). Since excited Rydberg Ps have significantly longer lifetime than ground state o-Ps, the laser excitation signal on SSPALS shots is first translated by a decrease in annihilation counts during the travel of Ps\* into vacuum, until they reach the test chamber walls and annihilate. At such long times ( $t \geq 300 \text{ ns}$ ), the SSPALS shows an increase of annihilation counts in case of laser ON, consistent with longer living Ps atoms and thus a Rydberg excitation signal.

Fig. 5 b) presents the Rydberg lines for  $n=15$  and  $n=16$  states. For higher  $n$ , the Zeeman and Stark effects induced by our field conditions imply a too strong mixing of the states to be able to distinguish them.

At resonance and for saturation regimes, the Rydberg excitation signal was found to be mainly limited by the laser bandwidth that defines the velocity range of Ps to match the resonance. The S parameter for the Rydberg signal has been calculated on an integration time window of  $300 \text{ ns} - 600 \text{ ns}$ , and gives another indirect proof of an efficient laser excitation of the  $n=3$  state.

## 6. Further improvements of $\bar{H}$ production via laser interactions.

Two keys ingredients to increase the formation rate of antihydrogen via charge-exchange would be: first, getting the antiproton plasma as cold as possible, and second, improving the overlap of the propagating Ps\* cloud and the trapped  $\bar{p}$  plasma. A possible laser-matter interaction has been considered to reach a colder antiproton plasma, or to focus the Ps beam and increase the solid angle



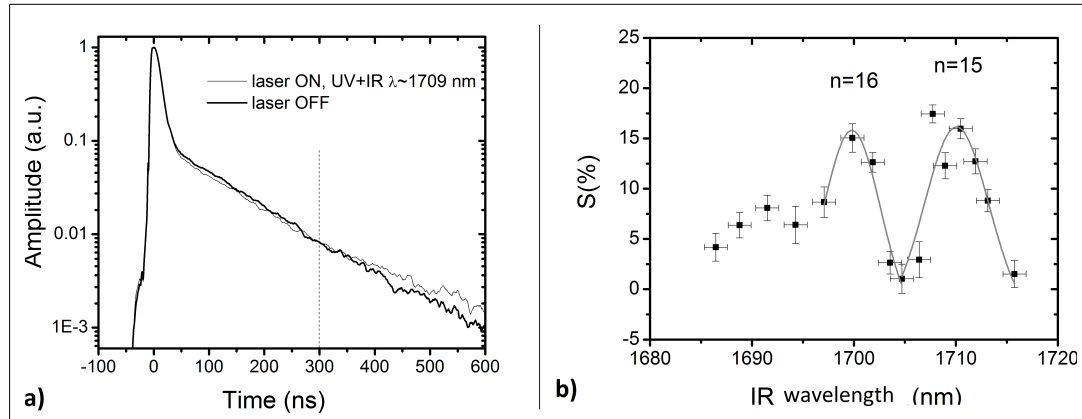


**Fig. 5.** a) Rydberg excitation SSPALS signal, for  $\lambda_{IR} = 1709$  nm, corresponding to the transition  $n=3 \leftrightarrow n=15$ . Lasers set at resonance.

b) Scan of the S parameter as function of the IR wavelength in the range  $n = 15 - 18$ . The grey curves are Gaussian fits of the  $n=15$  and  $n=16$  states. Results published in [20]

of the reaction, that we briefly discuss in this last section.

### 6.1 Towards a cold antiproton plasma

In the AEgIS proposal, a temperature of 100 mK is assumed to form efficiently a cold beam of antihydrogen atoms to perform gravity tests. To do so, a foreseen possibility is to use cold anions to sympathetically cool the antiproton plasma and laser cooling of anions is under study in AEgIS. The group of A. Kellerbauer has studied the spectroscopy of atomic anions, as  $\text{Os}^-$  [29] and  $\text{La}^-$  [30] to find the proper candidate, and a laser cooling scheme is under development for  $\text{La}^-$ .

A parallel study plans to use molecular anions instead of atomic anions. One major problem for applying laser cooling to molecules is to find a closed cycle of transitions, in order to avoid to populate dark states that would stop the cooling process. Although it has already been successfully performed for neutral diatomic molecules [28], it has never been done so far for anions. However, this project has the great advantage to provide a larger list of possible candidates. More specifically, one molecule has been recently selected: the  $\text{C}_2^-$  anion that presents a well known spectroscopy as well as good Franck-Condon coefficients (FC) to close with few lasers its transition  $X \leftrightarrow B$  (see Fig. 6 a), green arrows scheme). This implies that a Doppler laser cooling could be possibly considered.

Besides, a scheme to apply a Sisyphus cooling on the transition  $X \leftrightarrow A$ , in a Penning-like trap with a gradient of magnetic potential has been studied, and simulation results are encouraging [31]. The simulations have been performed using a C++ code that derives the evolutions of the external states (position and velocity) and internal states (internal level) of a cloud of particles under external forces, using the rate equations for stimulated absorption/emission, spontaneous decay and momentum recoil. The N-body Colombian interactions, the Lorentz and gravity forces are taken into account. A full description of the code can be found in [22]. In Fig. 6 b), the evolution of the axial temperature of the 200  $\text{C}_2^-$ , initialized with a Boltzmann distribution at 100 K, is presented. The particles confined into the Penning-like trap climb potential hill generated by Zeeman effect, and loose energy during the process. Cooling lasers are judiciously placed to transfer the particles down to the bottom's hill. More details about the Sisyphus cooling cycle can be found in [31]. The simulations indicate that the cloud of  $\text{C}_2^-$  can be cooled to few Kelvin in 80 ms.

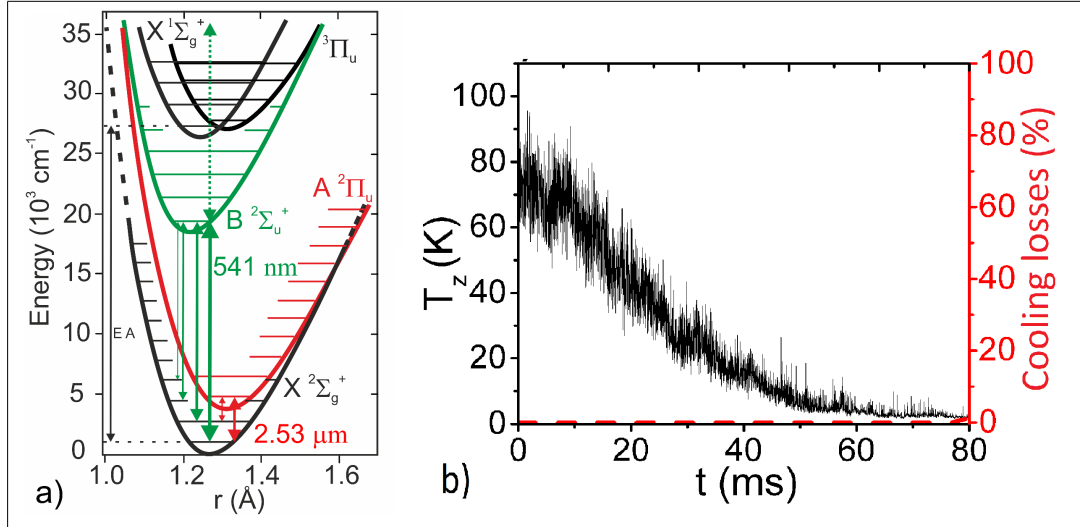


**Fig. 6.**  $C_2^-$  level structure and simulation results of Sisyphus laser cooling. a) Electronic and vibrational levels, as well as the optical transitions for a potential laser cooling are drawn. The green arrows show the Doppler cooling scheme on the  $X \leftrightarrow B$  transition, with a possible photodetachment (dashed green line). The red arrows point out the transitions that could be used for a Sisyphus cooling on the  $X \leftrightarrow A$  transition. The widths of the arrows are proportional to the transition strengths given by the Franck-Condon coefficients b) Evolution of the axial temperature (black) and number of  $C_2^-$  lost (red dashes), starting from an initial temperature of 100 K in an inhomogeneous Penning trap and cooled on the  $X \leftrightarrow A$  transition, with a repumping of the  $X(v'' = 1)$  losses [31].

The development of the test-setup has started recently at CERN. The small mass ratio between  $C_2^-$  atoms and  $\bar{p}$  seems to be promising for an efficient sympathetic cooling of the antiprotons, as studied in [32].

### 6.2 A possible laser Doppler cooling of Ps ?

In order to increase the antihydrogen formation rate in the AEGIS setup, it would be interesting to focus the Ps cloud that has to travel around 2 cm before reaching the antiproton plasma. For this purpose, a Doppler laser cooling of o-Ps has been studied on the transition  $1^3S \leftrightarrow 2^3P$ . This cooling process has been first studied by [23], and led to non conclusive experimental trials [24, 25]. A recent publication [26] proposes a new method to cool Ps in order to reach a BEC. We present here simulation results of the Doppler cooling of o-Ps, performed to determine its feasibility within the AEGIS apparatus, with the dye-based laser systems we have. The same C++ code as in Sec. 6.1 has been used.

The short lifetime of Ps ( $\tau_{o-Ps} = 142$  ns) is one of the main constraints. If we want to laser cool the Ps on its first transition, it has to occur within tens of ns ; where the usual Doppler cooling constant times are rather in the order of tens of ms. Positronium however has the advantageous property of being the lightest atom, composed of an electron and its antiparticle of same mass, the positron. The energy recoil resulting from the absorption of a single photon is then considerably more important than for usual atoms. A useful cycle of absorption - spontaneous emission means a velocity changes

of  $v_{recoil} = \frac{h}{2m_e \lambda} \approx 1500 \text{ m.s}^{-1}$ , for the laser wavelength  $\lambda = 243. \text{ nm}$  This property compensates for the short time constraints, since in few tens of cycles a considerable energy can be removed from the Ps.



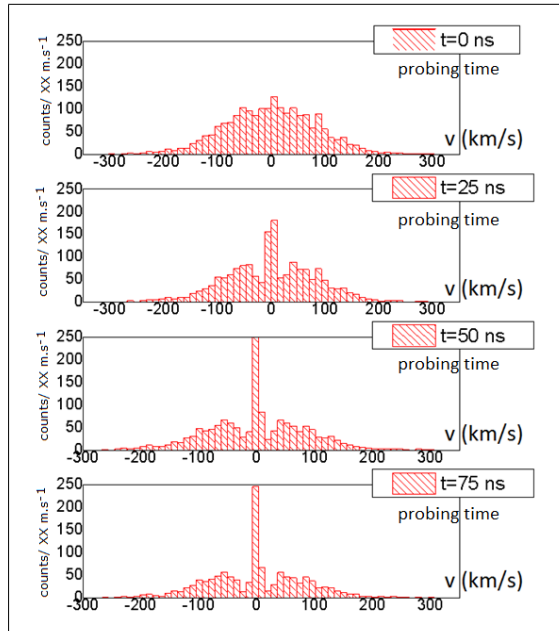


Fig. 7 1D Doppler laser cooling simulations, in free field. The velocity distributions of a cloud of 2000 Ps, initially at 1000 K (Maxwell-Boltzmann distribution), are shown for different times of laser interaction. The top a) is probed just before the laser cooling starts ( $t=0$  ns). The following b), c) and d) show the evolution of the distribution of the velocities during the cooling process. The atoms excited by lasers get cooler, implying a reduction of the number of atoms in the velocity range in resonance with the lasers, indicated by the two black arrows. This leads to an increase of the central counts, meaning an increase of the numbers of slow atoms ( $v \approx 0$  m.s<sup>-1</sup>).

Careful checks have been taken to model such special Doppler cooling, where the huge energy recoil perturbs the hypothesis of Brownian movement formalism usually used to calculate the Doppler cooling strength via the radiation pressure force. Simulations have been carried out and seem to indicate a possible effective cooling in tens of ns. In Fig. 7, the simulated 1D velocity distribution of 2000 Ps is presented, probed for different times during the laser interaction. The Ps cloud is generated to have an initial temperature of 1000 K, following a Maxwell-Boltzmann distribution.

The top histogram Fig.7 a) shows the Ps distribution before the cooling starts. The two counter-propagating Gaussian lasers address a limited velocity range at a detuning of  $2.5$  cm<sup>-1</sup>, indicated by the two black arrows in Fig.7 a). The bandwidth of the lasers has been set at  $\Gamma_L = 50$  GHz, rms value. During the cooling process, the atoms in the velocity range at resonance with the lasers are depopulated, and the number of atoms around  $v \approx 0$  m.s<sup>-1</sup> increases, as shown in the b), c) and d) distributions. At 50 ns, a clear increase of the number of the slow Ps atoms is visible (central peak at the zero velocity ranges enhanced). After 75 ns of cooling, we can notice that the annihilation process starts to be visible: despite the laser cooling that continues to populate the zero-velocity range of the Ps cloud's velocity distribution, the central peak decreases due to the o-Ps annihilation in vacuum. The simulations have been performed for a thermal cloud of 2000 Ps at an initial temperature of 1000 K, and for a laser power of 5000 W, with 7 mm of waist (Gaussian distribution), leading to a moderate saturation of the optical transition.

Another refinement must be taken into account in the presence of a high magnetic field that mixes the triplet excited states with singlet state. This mixing allows fast decays toward the p-Ps ground states that annihilates in 125 ps. This could be avoided by playing on the lasers' polarization to only excite pure states and keep a closed cycle of absorptions and emissions. But this solution limits the Doppler cooling to be performed only along the magnetic axis. Fortunately, this should be applicable for the AEgIS setup since we aim to cool the transverse velocity of the emitted Ps that corresponds to the direction of the 1 T magnetic field of the Penning-Malmberg traps, in order to focus the cloud in one dimension.

Laser developments are under study, since a rather long intense laser pulse is required to effectively cool the atoms. More details about these simulations, and the experimental work carried out

can be found in [33].

## 7. Summary and prospects

The presented measurements are the first observation of the  $n=3$  Ps laser excited state and the demonstration of another efficient optical path to reach  $\text{Ps}^*$  Rydberg states. These results represent a significant progress toward the formation of antihydrogen for the AEGIS experiment and, we believe, have a larger interest for the antimatter community. For instance, the GBAR collaboration considers a possible use of the  $n=3$  Ps state to enhance their antihydrogen formation rate [27].

Possible improvements for the antihydrogen creation rate have been studied using laser-matter interaction solutions for both cooling antiproton plasmas and focusing Ps clouds, that could open paths to even more precise measurements as for instance gravity test on Ps [34, 35].

## 8. Acknowledgments

This work was supported by: Istituto Nazionale di Fisica Nucleare (INFN-Italy), DFG research grant, excellence initiative of Heidelberg University, ERC under the European Unions Seventh Framework Program (FP7/2007-2013) ERC Grant agreement no. (291242) and no. (277762), Austrian Ministry for Science, Research and Economy, Research Council of Norway, Bergen Research Foundation, John Templeton Foundation, Ministry of Education and Science of the Russian Federation and Russian Academy of Sciences, European social fund within the framework of realizing the project: Support of inter-sectoral mobility and quality enhancement of research teams at Czech Technical University in Prague, CZ.1.07/2.3.00/30.0034.

## References

- [1] S.G. Karshenboim: Phys. Rep. **422** (2005) 1 - 63
- [2] E.G.Adelberger, J.H.Gundlach, B.R.Heckel, S.Hoedl, and S.Schlaminger: Prog. Part. Nucl. Phys. **62** (2009) 102 - 134
- [3] S. Pakvasa, W.A. Simmons and T.J. Weiler: Phys. Rev. D **39** (1989) 1761–1763
- [4] A Apostolakis et al: Phys. Lett. B **452** (1999) 425 - 433
- [5] M. M. Nieto and T. Goldman: Phys. Rep. **205** (1991) 221 - 281
- [6] J. Ponce de Leon: Int. J. Mod. Phys. D **18** (2009) 251-273
- [7] M. Amoretti et al: Nature. **419** (2002) 456-459
- [8] G. Gabrielse, et al.: Phys. Rev. Lett. **89** (2002) 233401
- [9] G. B. Andresen, et al: Nature **468** (2010) 673
- [10] P. Debu: J. Phys.: Conf. Ser. **460** (2013) 012008
- [11] C. Amole, et al: Nat. Commun **4** (2013) 1785
- [12] M. Doser et al.: Class. Quantum Grav. **29** (2012) 184009
- [13] C. H. Storry et al.: Phys. Rev. Lett. **93** (2004) 263401
- [14] S.Aghion et al: Nat. Commun. **5** (2014) 4538
- [15] M. L. Wall, C. S. Norton, and F. Robicheaux: Phys. Rev. A **72** (2005) 052702
- [16] S.Aghion et al: Nucl. Inst. Meth. Phys. R. B **362** (2015) 86 - 92
- [17] D. B. Cassidy, S. H. M. Deng, H. K. M. Tanaka, and A. P. Mills,Jr: Appl. Phys. Lett. **88** (2006) 19
- [18] D. B. Cassidy, T. H. Hisakado, H. W. K. Tom, and A. P. Mills: Phys. Rev. Lett. **108** (2012) 043401
- [19] S. Cialdi , et al: Nucl. Instrum. Methods. Phys. Res. B **269** (2011) 15271533
- [20] S. Aghion et al.: Phys. Rev. A **94** (2016) 012507
- [21] S. Mariuzzi, P. Bettotti, and R. S. Brusa: Phys. Rev. Lett. **104** (2010) 243401
- [22] D. Comparat: Phys. Rev. A. **89** (2014) 043410
- [23] E. P. Liang and C. D. Dermer: Optics Comm. **65** (1988) 419-424
- [24] H Iijima, T Asonuma, T Hirose, M Irako, T Kumita, M Kajita, K Matsuzawa, and KWada: Instru. Meth. Phys. Res. A **455** (2000) 104-108

- [25] T. Kumita, T. Hirose, M. Irako, K. Kadoya, B. Matsumoto, K. Wada, N.N. Mondal, H. Yabu, K. Kobayashi, and M. Kajita: Nucl. Instru. Meth. Phys. Res. B, **192** (2002) 171 -175
- [26] K Shu and X Fan and T Yamazaki and T Namba and S Asai and K Yoshioka and M Kuwata-Gonokami: J. Phys. B: At. Mol. Opt. Phys. **49** (2016) 104001
- [27] A.S. Kadyrov, C.M. Rawlins, A.T. Stelbovics, I. Bray, and M. Charlton: Phys. Rev. Lett. **114** (2015) 183201.
- [28] E. S. Shuman, J. F. Barry and D. DeMille: Nature Lett. **467** (2010) 820 - 823
- [29] A. Kellerbauer and S.Fritzsche: J. Phys.: Conf. Ser. **388** (2012) 012023
- [30] E. Jordan, G.Cerchiari, S. Fritzsche and A. Kellerbauer: Phys. Rev. Lett. **115** (2015) 113001
- [31] P. Yzombard, M. Hamamda, S. Gerber, M. Doser, D. Comparat: Phys. Rev. Lett. **114** (2015) 213001
- [32] L. Hilico, J-P. Karr, A. Douillet, P. Indelicato, S. Wolf, and F. Schmidt Kaler: arXiv **1402.1695** (2014)
- [33] P. Yzombard : Ph.D thesis - T.E.L. **2016SACLS272** (2016) tel-01446588
- [34] M.K. Oberthaler: Nucl. Instr. Meth. Phys. Res. B **192** (2002) 129
- [35] G. Dufour, D. B. Cassidy, P. Crivelli, et al: Advances in High Energy Physics, **2015** (2015) 379642